

Collective modes in metallic photonic crystals with subwavelength grooves

Ruey-Lin Chern^{1,*} and Yung-Chiang Lan²¹*Institute of Applied Mechanics, National Taiwan University, Taipei 106, Taiwan, Republic of China*²*Institute of Electro-Optical Science and Engineering, National Cheng Kung University, Tainan 701, Taiwan, Republic of China*

(Received 30 March 2009; published 23 July 2009)

We investigate collective modes in metallic photonic crystals with subwavelength grooves. A large number of frequency branches appear for TE polarization, which possess similar dispersion features of surface plasmons that occur in plasmonic structures. These modes are dispersionless in nature and intensively gathered around an asymptotic frequency that depends solely on the groove height. The typical collective modes are illustrated with the localized magnetic field patterns at the resonant frequencies. In particular, the field distribution in each groove shows a close resemblance to the TE_{n0} mode of an open-ended waveguide. The respective cutoff frequency serves as the asymptotic frequency of collective modes.

DOI: 10.1103/PhysRevB.80.033107

PACS number(s): 41.20.Jb, 42.70.Qs, 78.20.Bh

I. INTRODUCTION

There has been a great deal of interest in the properties of plasmonic structures, where the coupling of photons and electrons gives rise to surface-plasmon polaritons.¹ These waves are collective excitations of electric charges coupled with the electromagnetic fields. Due to the evanescent nature, the field intensities of surface plasmons are largely confined and strongly enhanced at the metal-dielectric interface. This feature has been explored in potential applications in nano-optics² and plasmonics,^{3,4} where the properties of photonics and electronics are merged at the subwavelength scale.

In periodically arranged structures such as plasmonic crystals, surface plasmons appear as collective modes.⁵⁻⁷ There exist a large number of resonant modes gathering around the so-called surface plasma frequency. These modes exhibit a highly degenerate nature; that is, different modes are oscillating at the same frequency. A similar feature appears as well in particle chains.^{8,9} Surface plasmons, however, do not exist in perfect metals. Although there would be an unlimited supply of free charges in such ideal conductors,¹⁰ the electromagnetic fields are completely expelled from the perfect metal and there are no states bound to the surface for sustaining plasma oscillations.

If the perfect-metal surface is perforated with subwavelength holes, the fields can somehow penetrate the (effective) surface. The subwavelength holes present themselves disturbances to a totally reflecting surface, which support electromagnetic bound states and give rise to the so-called surface-plasmonlike modes.¹¹ In particular, these surface modes exhibit similar dispersion relations with those of real surface plasmons. This feature has been illuminated from the skin-depth point of view.¹² In addition, the fields in the vicinity of a subwavelength hole are effectively represented by an electric dipole perpendicular to the surface and a magnetic dipole parallel to it.¹³ This dipolar nature was also demonstrated with the surface electric field measurements.¹⁴

In another aspect, surface-plasmonlike modes were identified as the eigenmodes associated with the subwavelength hole structures.^{15,16} As the solutions of Maxwell's equations are scale invariant for perfect conductors,¹⁷ characteristics of surface-plasmonlike modes are dependent solely on the hole geometry and can, therefore, be engineered to a variety of frequency ranges.¹¹ For this reason, surface-plasmonlike

modes are also named designer surface plasmons.^{18,19} As these waves are unusual to nonplasmonic materials, the metallic structures with subwavelength holes are regarded as plasmonic metamaterials.^{20,21}

In this study, we investigate collective modes in metallic photonic crystals with subwavelength grooves. These collective modes possess similar dispersion features of surface plasmons in two aspects. First, a large number of frequency branches appear and gather around an asymptotic frequency for TE polarization, which are similar to surface-plasmon modes that occur in plasmonic structures. Second, the typical resonant modes exhibit a highly localized field distribution within the grooves, outside which the field amplitudes are rapidly decayed. This is another distinguished feature of surface plasmons. In particular, the magnetic fields in each groove retain a similar pattern, which is analogous to TE_{n0} mode of an open-ended waveguide. The respective cutoff frequency serves the role of asymptotic frequency for collective modes. These collective modes give rise to flattened bands with high density of states and small group velocities near certain frequencies, which suggest the potential applications in sensing, signal processing, and communication.

II. BASIC EQUATIONS

Consider a two-dimensional photonic crystal composed of a periodic array of perfect-metal cylinders. A certain number of rectangular grooves, basically on the subwavelength scale, are milled on the cylinder surface. Figure 1 shows the sche-

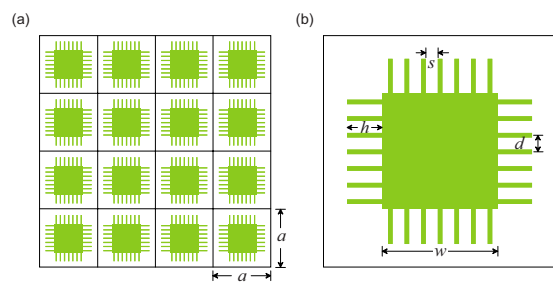


FIG. 1. (Color online) Schematics of (a) the metallic photonic crystal with subwavelength grooves and (b) the groove structure in the unit cell. The shaded area denotes the perfect-metal region.

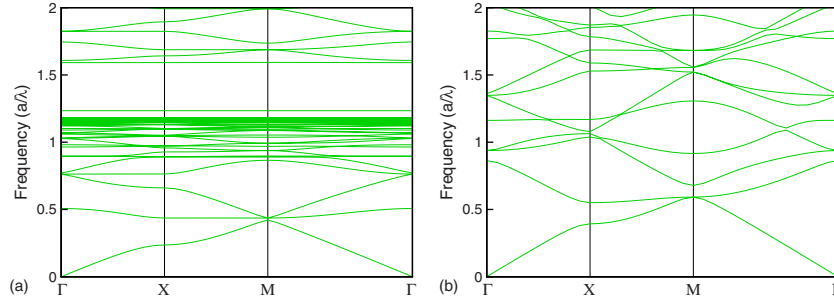


FIG. 2. (Color online) Dispersion diagram of the metallic photonic crystal (a) with subwavelength grooves, where $w/a=0.4$, $h/a=0.2$, $d/a=0.04$, and $s/a=0.03$, and (b) without subwavelength grooves, where $w/a=0.4$ and $h=d=s=0$.

matrics of the photonic crystal and the subwavelength groove structure in the unit cell. The basic thinking is to devise a mechanism for trapping electromagnetic fields at the subwavelength scale so that collective modes may arise due to the oscillation of fields at that scale. A simple way to fulfill this idea in photonic crystals is to construct a certain number of grooves on each surface of the cylinder, with the groove width being much smaller than the lattice constant. The ratio of groove height to groove width is chosen to be large so that the collective modes may occur at the frequency range which is of primary interest for ordinary photonic crystals. In this configuration, the interaction of electromagnetic waves with subwavelength grooves is responsible for the existence of collective modes in a perfect-metal structure. Basic features of collective modes are either manifest or implied in the dispersion characteristics. As in the case of surface plasmons, these collective modes occur in TE polarization, where the magnetic fields are oriented along the cylinder axis. In this polarization, the electric fields normal to the metal surface give rise to surface charges for sustaining plasma oscillations.

For propagation of waves parallel to the lattice plane, the time-harmonic magnetic mode (with time dependence $e^{-i\omega t}$) is described by

$$-\nabla \cdot \left(\frac{1}{\varepsilon} \nabla H \right) = \left(\frac{\omega}{c} \right)^2 H. \quad (1)$$

Inside the perfect metal, the fields are identically zero ($H=0$). At the interface between the metal and surrounding dielectric material, the boundary condition is given by $\partial H / \partial n = 0$.²² The dielectric constant of the surrounding material is chosen as $\varepsilon=1$. For periodic structures with infinite extent, it is sufficient to solve the problem in one unit cell, along with the Bloch condition

$$H(\mathbf{r} + \mathbf{a}_i) = e^{i\mathbf{k} \cdot \mathbf{a}_i} H(\mathbf{r}) \quad (2)$$

applying at the unit-cell boundary, where \mathbf{k} is the Bloch wave vector and $\mathbf{a}_i (i=1,2)$ is the lattice translation vector. For photonic crystals with a delicate substructure, the dispersion relations can be efficiently solved by the inverse iteration method.^{23–25} The eigensystem, Eq. (1), is solved by making good use of the *Hermitian* property of the differential operator. An arbitrary distribution of fields over the unit cell is given as the initial guess of the eigenfunction and the Rayleigh quotient

$$Q = \frac{\int_{\frac{1}{\varepsilon}} |\nabla H|^2 d\tau}{\int |H|^2 d\tau} \quad (3)$$

is employed to calculate the eigenfrequency. By repeatedly solving the matrix inversion, the solution is refined through iterations until it is converged. The details of this approach can be found in Ref. 23

III. RESULTS AND DISCUSSION

A. Collective frequency branches

Figure 2(a) shows the dispersion diagram of a metallic photonic crystal with subwavelength grooves, where $w/a=0.4$, $h/a=0.2$, $d/a=0.04$, and $s/a=0.03$. A large number of frequency branches appear within a small frequency interval for TE polarization. As the frequency gets closer to $a/\lambda \approx 1.18$, more branches are observed. These collective modes have similar dispersion features of surface-plasmon modes that occur in plasmonic structures.^{7,26,27} They are dispersionless in nature; that is, their frequencies are insensitive to the change in wave vector. As a result, the corresponding frequency branches tend to be flattened. For real surface plasmons, the dispersionless nature comes from the strong coupling of photons with electrons in the plasmonic material. As the metals are treated as perfectly conducting materials in this study, there is no such coupling behavior. In fact, the electromagnetic mode at the perfect-metal surface is simply a surface current.¹⁸ No states are bound to the surface for sustaining plasma oscillations. For comparison, the dispersion diagram of the photonic crystal without subwavelength grooves is plotted in Fig. 2(b), where $w/a=0.4$ and $h=d=s=0$. This diagram depicts the usual dispersion for ordinary photonic crystals and no collective modes are observed.

For the present problem, the dispersionless nature comes from the interaction of waves with the subwavelength structure. The grooves serve as a mechanism for maintaining electromagnetic bound states so that collective modes may occur over the grooves. There exists an asymptotic frequency around which the collective modes are gathered. As in the case of subwavelength holes, this frequency is dependent on the groove geometry only. Figure 3 shows the variations in major collective modes with respect to four geometric parameters: the groove height h , groove width s , groove period d , and cylinder width w . It is shown in Fig. 3(a) that collec-

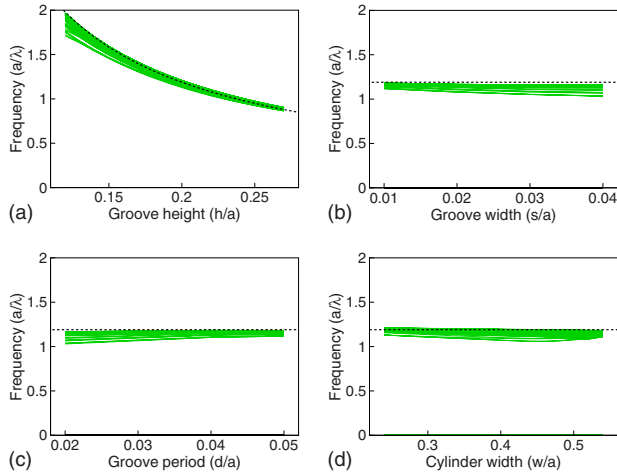


FIG. 3. (Color online) Variations in major collective modes with respect to (a) groove height h , where $w/a=0.4$, $d/a=0.02$, and $s/a=0.01$, (b) groove width s , where $w/a=0.4$, $h/a=0.2$, and $d/a=0.05$, (c) groove period d , where $w/a=0.4$, $h/a=0.2$, and $s/a=0.01$, and (d) cylinder width w , where $h/a=0.2$, $d/a=0.02$, and $s/a=0.01$. The dashed line denotes the asymptotic frequency of collective modes.

tive modes move to lower frequencies as the groove height increases. In particular, the asymptotic frequency of collective modes (denoted by the dashed line) is inversely proportional to the groove height. On the other hand, the collective modes are less affected by the other three parameters. In Figs. 3(b)–3(d), the groove height is held fixed and the asymptotic frequency remains unchanged with respect to groove width, groove period, and cylinder width.

B. Localized eigenmodes

The features of collective modes are further illustrated with the resonant field patterns. Figure 4(a) shows the magnetic field contours of a typical resonant mode at $a/\lambda \approx 1.18$ for the metallic photonic crystal with subwavelength grooves, where $w/a=0.4$, $h/a=0.2$, $d/a=0.04$, and $s/a=0.03$. Note that the fields are highly localized inside the grooves and rapidly decayed outside. This is another distinguished feature of surface-plasmon modes that appear in plasmonic structures.^{7,26,27} Due to localization, the interac-

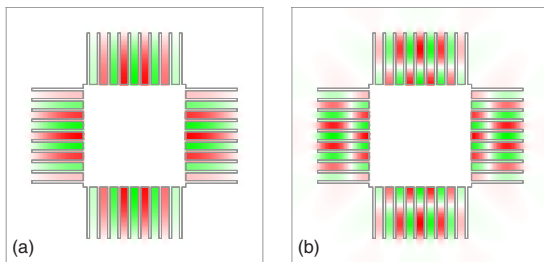


FIG. 4. (Color online) Magnetic field contours of two typical collective modes at (a) $a/\lambda \approx 1.18$ and (b) $a/\lambda \approx 3.53$ for the metallic photonic crystal with subwavelength grooves, where $w/a=0.4$, $h/a=0.2$, $d/a=0.04$, and $s/a=0.03$. Red (dark gray) and green (light gray) colors denote the positive and negative field values, respectively.

tion of fields inside the grooves with those outside is rather weak. The resonant frequency is therefore insensitive to the change in wave vector and the branches become flattened or dispersionless (cf. Figure 2). In particular, the magnetic fields in each groove retain a similar pattern and the field orientations are alternate over adjacent grooves. This feature indicates that the coupling of fields between grooves is small and the resonant modes possess a high degeneracy; that is, different modes oscillate at the same frequency. As the number of grooves increases, the high degenerate nature becomes more evident. This is consistent with the appearance of a large number of collective modes within a small frequency interval.

In addition to the collective mode in Fig. 4(a), a similar resonant mode occurs at a much higher frequency $a/\lambda \approx 3.53$ for the same photonic crystal as shown in Fig. 4(b). Note that the fields are also localized inside the grooves but with a different oscillation pattern. A nodal point (with zero field) exists in each groove at about one third of the groove height from the groove bottom. Besides, the resonant frequency is approximately three times larger. The resonant mode in Fig. 4(b) is therefore considered a high-order collective mode for the subwavelength groove structure. These modes also appear as flattened bands whose frequencies are insensitive to the change in wave vector. A minor difference is that the high-order collective modes spread a slightly wider band width due to a somewhat complex coupling of fields between the grooves.

C. Open-ended waveguides

The features of collective modes stated above can be characterized by the properties of an open-ended waveguide. Consider a rectangular waveguide of height h and width s , where the top end is left opened. For TE polarization ($E_z=0$), the H_z field in the waveguide satisfies the Helmholtz equation $(\nabla^2+k^2)H_z=0$, where k is the wave number. The perfect-metal boundary condition gives $\partial H_z/\partial n=0$ on the left, right, and bottom sides. On the top end, the H_z field is assumed to behave like $H_z \propto e^{-\gamma y}$, where γ is a decay factor, so that the fields are exponentially decayed away from the open end (the condition of a bound state). Accordingly, the boundary condition is written as $\partial H_z/\partial n + \gamma H_z=0$. The solution of H_z is given by

$$H_z(x,y) = A_{nm} \cos(\alpha_n y) \cos\left(\frac{m\pi x}{s}\right),$$

$$n = 1, 2, \dots, \quad m = 0, 1, 2, \dots, \quad (4)$$

where A_{nm} is an arbitrary amplitude constant and α_n is the n th root of

$$\alpha \tan(\alpha h) = \gamma. \quad (5)$$

Numerical solutions of α_n for $n=1, 2$ are plotted in Fig. 5(a). As γ increases, α_1 and α_2 asymptotically approach $\frac{\pi}{2h}$ and $\frac{3\pi}{2h}$, respectively.

In the neighborhood of an asymptotic value, the approximate solution of α_n can be obtained by use of Taylor's expansion; for example, $x \tan(x) \approx -\frac{\pi}{2}(x - \frac{\pi}{2})^{-1} - 1 + \frac{\pi}{6}(x - \frac{\pi}{2})$ or

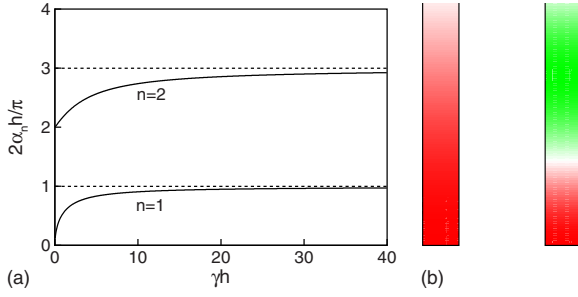


FIG. 5. (Color online) (a) Solutions of α_n in Eq. (5) for $n = 1, 2$. (b) Field patterns of TE_{10} mode (left) and TE_{20} mode (right) of an open-ended waveguide, where $s/h=0.15$ and $\gamma h=20$.

$x \tan(x) \approx -\frac{3\pi}{2}(x - \frac{3\pi}{2})^{-1} - 1 + \frac{\pi}{2}(x - \frac{3\pi}{2})$. The expansion gives rise to $\alpha_1 \approx \frac{\pi}{2h}(1 - \frac{1}{\gamma h})$, $\alpha_2 \approx \frac{3\pi}{2h}(1 - \frac{1}{\gamma h})$, and so forth. If the height h is substantially larger than the width s , the H_z field of the dominate TE_{n0} mode is approximated as

$$H_z(x, y) \approx A_{n0} \cos\left[\frac{(2n-1)\pi}{2h}\left(1 - \frac{1}{\gamma h}\right)y\right], \quad (6)$$

and the respective cutoff frequency is given by

$$f_{c_{n0}} \approx \frac{(2n-1)c}{4h}\left(1 - \frac{1}{\gamma h}\right). \quad (7)$$

Let the open-ended waveguide have the same geometry of the subwavelength groove and the decay factor γ be sufficiently large. For $\gamma h=20$ and $h/a=0.2$, we have $f_{c_{10}} \approx 1.19c/a$ and $f_{c_{20}} \approx 3.56c/a$, which are close to the resonant frequencies $a/\lambda \approx 1.18$ and 3.53 for the two typical collective modes of the metallic photonic crystal with subwavelength grooves (cf. Figure 4). In particular, the H_z fields of TE_{10} and TE_{20} modes, plotted in Fig. 5(b), have a close resemblance to the magnetic field patterns inside the groove

for the two collective modes. These features indicate that the subwavelength groove acts like an open-ended waveguide at the resonant frequencies. In addition, we have from Eq. (7) that $f_{c_{n0}} \propto \frac{1}{h}$. This clarifies that the asymptotic frequency of collective modes is inversely proportional to the groove height and not affected by the change in groove width, groove period, and cylinder width (cf. Figure 3).

IV. CONCLUDING REMARKS

In conclusion, the collective modes in metallic photonic crystals with subwavelength grooves have been investigated. The groove structure serves as a mechanism for sustaining electromagnetic bound states in the perfect-metal structure. Existence of collective modes is manifest on the intensively gathered frequency branches and localized field patterns for TE polarization. At the resonant frequencies, each subwavelength groove acts like an open-ended waveguide with regard to the mode pattern and cutoff frequency. As the properties of collective modes share some common features of surface plasmons that occur in plasmonic structures and can be engineered by the groove geometry, the metallic photonic crystals with subwavelength grooves are eligible to be plasmonic metamaterials. For real metals, the electromagnetic fields no longer vanish inside the structure and two important effects will alter the overall dispersion characteristics. The effect of dissipation results in a decay factor (in time) of the resonant modes and the effect of skin depth may give rise to surface plasmons.²⁸ In particular, if the surface modes happen to occur near the frequency of collective modes, it is expected that the dispersion bands will exhibit a very different and complex character.

This work was supported in part by the National Science Council of the Republic of China under Contracts No. NSC 96-2221-E-002-190-MY3 and No. NSC 97-2120-M-002-013.

*chern@iam.ntu.edu.tw

¹W. Barnes, A. Dereux, and T. Ebbesen, *Nature (London)* **424**, 824 (2003).

²A. V. Zayats, I. I. Smolyaninov, and A. A. Maradudin, *Phys. Rep.* **408**, 131 (2005).

³E. Ozbay, *Science* **311**, 189 (2006).

⁴S. A. Maier, *Plasmonics: Fundamentals and Applications* (Springer, New York, 2007).

⁵T. Ito and K. Sakoda, *Phys. Rev. B* **64**, 045117 (2001).

⁶E. Moreno, D. Erni, and C. Hafner, *Phys. Rev. B* **65**, 155120 (2002).

⁷R. L. Chern, C. C. Chang, and C. C. Chang, *Phys. Rev. E* **73**, 036605 (2006).

⁸S. A. Maier, P. G. Kik, and H. A. Atwater, *Appl. Phys. Lett.* **81**, 1714 (2002).

⁹S. Y. Park and D. Stroud, *Phys. Rev. B* **69**, 125418 (2004).

¹⁰D. J. Griffiths, *Introduction to Electrodynamics*, 3rd ed. (Prentice-Hall, New Jersey, 1999).

¹¹J. B. Pendry, L. Martin-Moreno, and F. J. Garcia-Vidal, *Science* **305**, 847 (2004).

¹²W. Barnes and R. Sambles, *Science* **305**, 785 (2004).

¹³F. J. Garcia de Abajo and J. J. Sáenz, *Phys. Rev. Lett.* **95**, 233901 (2005).

¹⁴B. Hou *et al.*, *Appl. Phys. Lett.* **89**, 131917 (2006).

¹⁵Y. C. Lan and R. L. Chern, *Opt. Express* **14**, 11339 (2006).

¹⁶L. Shen, X. Chen, and T. J. Yang, *Opt. Express* **16**, 3326 (2008).

¹⁷L. Martin-Moreno and F. García-Vidal, *Opt. Express* **12**, 3619 (2004).

¹⁸A. P. Hibbins, B. R. Evans, and J. R. Sambles, *Science* **308**, 670 (2005).

¹⁹A. P. Hibbins *et al.*, *Opt. Express* **16**, 20441 (2008).

²⁰F. J. Garcia-Vidal, L. Martin-Moreno, and J. B. Pendry, *J. Opt. A, Pure Appl. Opt.* **7**, S97 (2005).

²¹A. P. Hibbins *et al.*, *Phys. Rev. Lett.* **96**, 073904 (2006).

²²J. D. Jackson, *Classical Electrodynamics*, 3rd ed. (Wiley, New York, 1999).

²³R. L. Chern *et al.*, *Phys. Rev. E* **68**, 026704 (2003).

²⁴C. C. Chang *et al.*, *Phys. Rev. B* **70**, 075108 (2004).

²⁵R. L. Chern and S. D. Chao, *Opt. Express* **16**, 16600 (2008).

²⁶R. L. Chern, *Phys. Rev. B* **77**, 045409 (2008).

²⁷R. L. Chern, *Phys. Rev. B* **78**, 085116 (2008).

²⁸R. L. Chern, *Phys. Rev. E* **79**, 017701 (2009).